A differential thermal study of the chlorites.

By Wm. Revell Phillips, B.S., M.S., Ph.D.

Department of Geology, Brigham Young University, Provo, Utah.

[Read 27 September 1962.]

Summary. Differential thermal analysis alone appears inadequate as a tool for distinguishing the many chlorite varieties; however, this process is capable of yielding much valuable information about the chlorites. The 7 Å septechlorite structure may be easily distinguished from the normal 14 Å chlorite structure. Two stages of dehydration, oxidation of ferrous iron, and structural collapse appear as endothermic and exothermic peaks on the D.T.A. chlorite curves. Septechlorites show only one, large dehydration stage, which leads directly to the structural breakdown. Iron oxidation accompanies the initial dehydration in both structural types, and the temperature at which dehydration begins is noticeably lowered by increasing ferrous iron content of the chlorite variety.

During the 1953–4 academic year the author gathered together, from widely scattered localities, a large number of mineral specimens, each reported to contain some mineral of the chlorite group. Twenty-six of these specimens yielded a true chlorite variety in sufficient quantity and of sufficient purity for the procedures to be described. Each purified chlorite specimen was chemically analysed, at the Utah Engineering Experiment Station, by two analysts[1] experienced in silicate analysis. The author further subjected the twenty-six chlorite specimens to detailed examination by X-ray diffraction and differential thermal analysis, and the optical properties and specific gravity were determined. All procedures were evaluated with regard to possible sources of error and the expected magnitude of such errors. From the mass of data thus acquired the author was able to evaluate the usefulness of each line of investigation as a tool for distinguishing the various chlorite varieties. Differential thermal analysis, although insufficient for varietal classification, yielded some interesting observations, which are the subject of the present paper.

Procedure.

The differential thermal unit used for this work was built at the University of Utah Experiment Station and contains a nicrome-wire-wound furnace controlled by a cam-driven variac. Mineral powders

[1] Dr. Harold R. Bradford and Mr. Walter Savournin.

TABLE I. Details of the chlorites examined. In the 'source' column, B.F.S. indicates material collected by Bronson F. Stringham of the University of Utah, and H–G material obtained from Hatfield-Goudey of Nevada.

No.	*Mineral name and locality.*	*Source.*	*Description.*
1	Clinochlore Gabbs, Nevada	U.S.N.M. 105600	Very pale tan, massive, fine-grained (few microns) aggregate with minor limonite.
2	Clinochlore Långban, Sweden	Wards	Salmon coloured, transparent micaceous sheets (up to ½ in.) with feldspar and dolomite.
3	Delessite Zlatousk, Siberia	Wards	Cream-coloured powder containing a few light yellow micaceous flakes.
4	Sheridanite Miles City, Montana	U.S.N.M. 94515	White, massive schistose chlorite (few microns) with a few iron stains.
5	Clinochlore Brewster, New York	Wards	Light bluish green flakes and sheets (to 1 in.) with rutile, K-feldspar, and ilmenite.
6	Diabantite Bingham, Utah	B.F.S.	Bluish green, massive, soapy aggregate (tens of microns) with clays and sulphides.
7	Clinochlore Hiawassee, Georgia	Wards	Dense mass of pale green micaceous flakes (to ½ in.) with limonite stains.
8	Kochubeïte Siskiyou Co., California	U.S.N.M. 104723	Tabular, pale lavender, micaceous fragments with no known associated minerals.
9	Rhodophyllite Eldorado Co., Colorado	Wards	Pale green, pseudohexagonal crystals (to ¼ in.), lavender edges, with black spinel and limonite.
10	Sheridanite West Chester, Penn.	Wards	Large, pale green sheets (to 3 in.) with minor muscovite and limonite.
11	Sheridanite Hartford Co., Maryland	Wards	Fine-grained (microns), dark metallic green aggregate with rutile, ilmenite, and feldspar.
12	Delessite Lenni, Pennsylvania	Wards	Light metallic green, flexible flakes (to ½ in.) with no known associated minerals.
13	Ripidolite (Prochlorite) Chester, Vermont	Wards	Dark green, fine-grained (microns) schistose aggregate with large pyrite and magnetite crystals.
14	Diabantite Goose Greek, Virginia	Wards	Dark olive-green, soapy, fine-grained (microns) schistone mass with feldspar and quartz.
15	Corundophilite Chester, Massachusetts	Wards	Dark green flakes (to ⅛ in.) with diaspore.
16	Diabantite Newington, Connecticut	Wards	Dark olive-green spherulites in basalt. Flakes to ⅛ in. associated with calcite.
17	Ripidolite (Prochlorite) Southbury, Connecticut	Wards	Dark green flakes (to ½ mm) with limonite stains.
18	Aphrosiderite Simplon Tunnel, Switzerland	H-G	Dark olive-green, pseudohexagonal crystals (to ⅛ in.) with pericline, quartz, and muscovite.
19	Aphrosiderite Dona Ana Co., New Mexico	Wards	Dark olive-green, fine-grained (to ½ mm) mass with feldspar and limonite stains.
20	Daphnite Michigamme, Michigan	Wards	Dark green pseudomorphs after garnet, with garnet and magnetite.
21	Klementite Goscheneralpe, Switzerland	Wards	Dark greenish brown, granular (microns) mass with feldspar and quartz.

TABLE I (*cont.*)

No.	*Mineral name and locality.*	*Source.*	*Description.*
22	Septekämmererite Lancaster, Pennsylvania	Wards	Pale green to lavender fibrous mass (to $\frac{1}{4}$ in.) with dolomite and picrolite.
23	Antigorite Antigorio Valley, Italy	U.S.N.M. R.4648	Pale green, brittle sheets (to 1 in.) with no known associated minerals.
24	Septekämmererite Selukwe, Southern Rhodesia	Wards	Reddish violet vein in massive chromite. Fibres (to $\frac{1}{2}$ in.) associated with dolomite.
25	Septeamesite Chester, Massachusetts	Wards	Pale bluish green, pseudohexagonal crystals with dark, massive emery.
26	Septeaphrosiderite Bayange, Moselle, France	U.S.N.M.	Grey-green, oolitic masses associated with calcite.

(< 200 mesh) were packed, by the flattened end of a glass rod, into cavities $\frac{1}{4}$ in. in diameter and $\frac{1}{2}$ in. long in a cylindrical nickel block, and cromel-alumel differential thermocouples measured any difference in temperature between inert alumina and the mineral to be examined.

Equal weights of the different minerals should yield thermal peaks the relative heights of which could be of considerable significance; however, it was found that, with the available equipment, the height of the various peaks was reproducible only within rather wide limits, and so only limited reliance was placed on this variable. The position of the various exothermic and endothermic peaks was found to be reproducible within $\pm$ 10° C.

Presentation of data.

The origin and nature of the twenty-six specimens used for this investigation are set out in table I. Important X-ray diffraction data appear in table II, and differential thermal curves of the twenty-six chlorites are shown in figs. 1, 2, and 3. Chemical analysis data are presented in table III. The chlorite variety names shown in the tables and text were assigned by the author in accord with his own method of chlorite classification.[1] Variety names agree with the system of Hey,[2] except numbers 8, 9, 14, 17, 18, 19, 20, 22, 23, 24, 25, and 26. Numbers 8 and 9 are high-chromium chlorites, and numbers 22, 23, 24, 25, and 26 are 7 Å septechlorites, none of which were named by Hey in his classification. Number 20 can be referred to Hey's diagram, but no name was given to this composition area. To numbers 14, 17, 18, and 19, Hey would assign the names delessite, thuringite, thuringite, and thuringite respectively. The author uses the names 'septeamesite,' 'septekämmererite', and 'septeaphrosiderite' advisedly and in harmony with the

[1] W. R. Phillips, unpublished Ph.D. thesis, 1954, University of Utah.
[2] M. H. Hey, Min. Mag., 1954, vol. 30, p. 277.

proposed nomenclature of Nelson and Roy.[1] The term 'septeantigorite' seems reasonable for consistency; however, the universally accepted name 'antigorite' is perhaps preferable and may be integrated with the 'septe-' prefix system, since the 14 Å analogue of antigorite does not exist.

TABLE II. X-ray powder data for chlorites (details in Table I).

No.	*Mineral name.*	d_{001}.	I/I_0.	d_{002}.	I/I_0.
1	Clinochlore	14·2 Å	0·8	7·06 Å	0·8
2	Clinochlore	14·1	0·9	7·10	1·0
3	Delessite	13·9	0·3	6·98	0·4
4	Sheridanite	14·2	0·7	7·06	0·9
5	Clinochlore	14·2	0·8	7·10	1·0
6	Diabantite	14·1	0·8	7·02	1·0
7	Clinochlore	14·1	0·8	7·02	0·9
8	Kochubeïte	14·4	0·8	7·14	1·0
9	Rhodophyllite	14·1	0·9	7·06	1·0
10	Sheridanite	14·2	0·7	7·06	1·0
11	Sheridanite	14·2	0·9	7·06	1·0
12	Delessite	14·4	1·0	7·14	0·5
13	Ripidolite	13·9	0·9	7·06	1·0
14	Diabantite	14·4	1·0	7·10	0·7
15	Corundophilite	13·9	0·8	6·98	1·0
16	Diabantite	14·2	0·8	7·10	1·0
17	Ripidolite	14·2	0·8	7·02	1·0
18	Aphrosiderite	13·9	0·8	6·98	1·0
19	Aphrosiderite	14·2	0·6	7·02	1·0
20	Daphnite	13·9	0·6	7·02	1·0
21	Klementite	14·2	0·9	7·02	1·0
22	Septekämmererite	7·21	1·0	3·59	0·8
23	Antigorite	7·17	1·0	3·58	0·8
24	Septekämmererite	7·14	1·0	3·56	0·8
25	Septeamesite	6·94	1·0	3·47	0·8
26	Septeaphrosiderite	7·14	0·8	3·58	0·8

Observations and conclusions.

The most casual observation of the differential thermal curves in figs. 1, 2, and 3 will call attention to the major conclusion of this report: Normal 14 Å chlorites (i.e. alternating 'brucite' and 'mica' layers) yield curves easily distinguishable from the 7 Å septechlorites (i.e. 'kaolinite' layers). Those chlorites shown by X-ray diffraction to possess the normal 14 Å structure consistently yield a thermal curve showing a large, broad endothermic peak at some temperature between 550° C and 675° C separated by a hundred degrees or more of inactivity from a smaller, narrow exothermic peak at some temperature between 805° C and 875° C.

[1] B. W. Nelson and R. Roy, Amer. Min., 1958, vol. 43, p. 707.

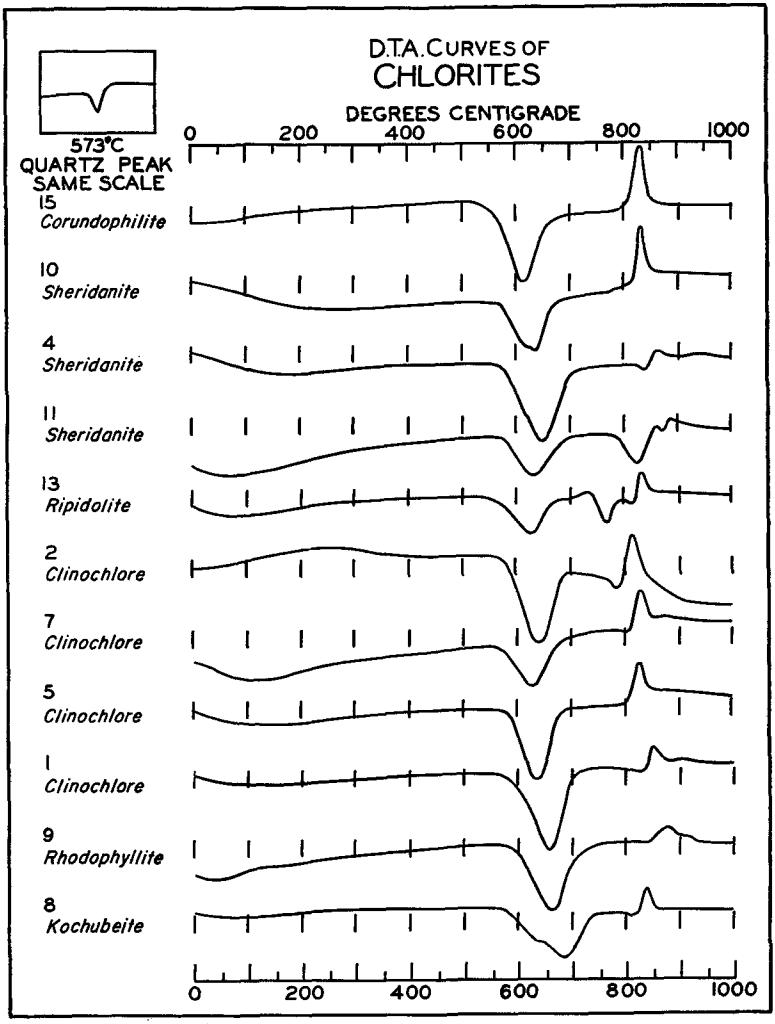

FIG. 1. Differential thermal analysis curves of normal chlorites.

A few 14 Å chlorites show a second endothermic peak at about 800° C, and still others show an endothermic reaction at a low temperature below 150° C.

Septechlorites, on the other hand, show a large, broad endothermic peak somewhere between 550° C and 750° C which passes directly into a sharp exothermic peak at about 800° C.

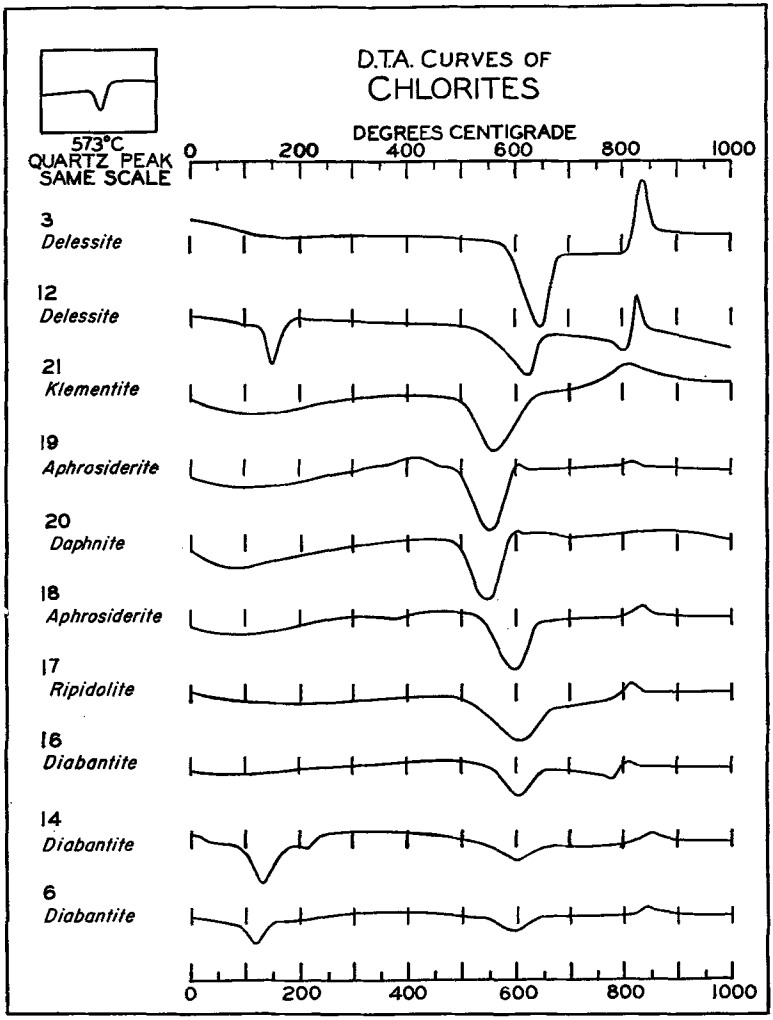

FIG. 2. Differential thermal analysis curves of normal chlorites.

The writer made some attempt to explain the observed reactions, and the following is offered as an interpretation thereof.

Endothermic reactions occurring below 200° C were considered to represent the loss of adsorbed water and were not deemed important to an understanding of the chlorites.

The characteristic exothermic peak occurring between 800° C and

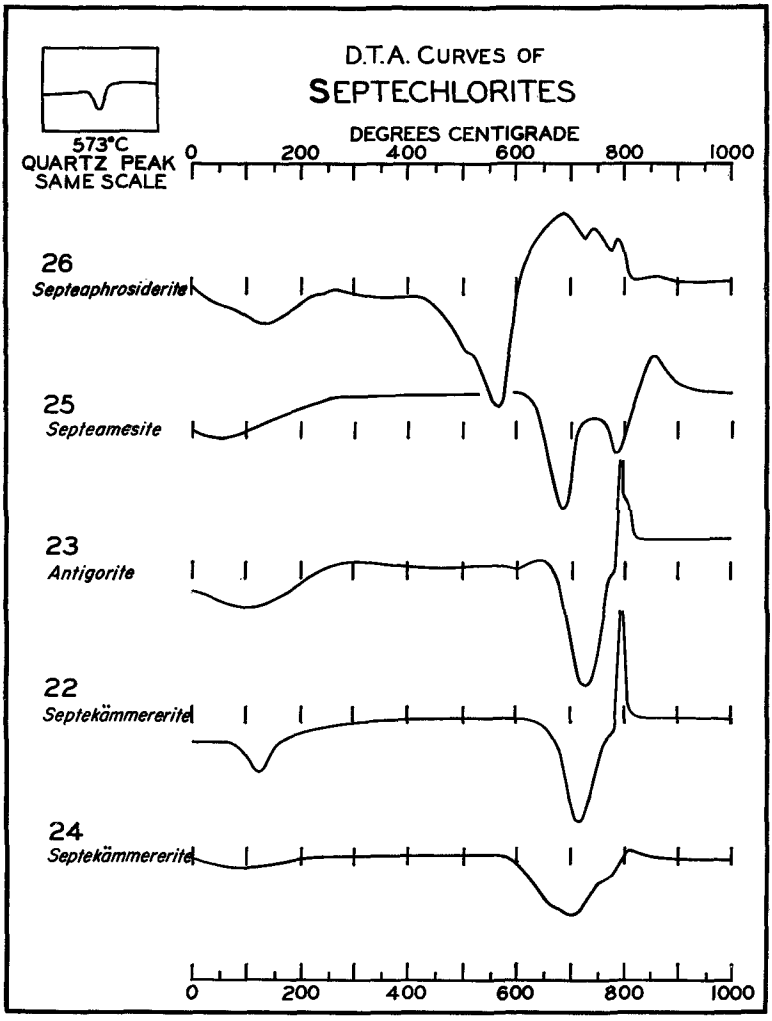

FIG. 3. Differential thermal analysis curves of septechlorites.

875° C appears to represent the breakdown of the chlorite structure, as indicated by X-ray powder patterns taken at various temperatures during the heating history. Immediately below the peak, X-ray diffraction shows a pattern recognizable as that of a chlorite structure, though the relative line intensities differ greatly from those of the unheated chlorite, with the 001 line becoming especially dark and conspicuous.

Above the peak, powder photographs show only a very few weak, diffuse lines suggestive of a simple isometric structure. This peak is narrow, indicating that, as one would expect, the structural adjustment occurs at a specific temperature and not over a wide temperature range.

The large, characteristic endothermic peak occurring at about 600° C for the 14 Å structure and at about 700° C for the 7 Å structure appears to represent dehydration of the chlorite proper, presumably with the replacement of OH′ ions by O″ ions. Chemical analysis of the corundophilite from Chester, Massachusetts, immediately following this peak showed this 14Å chlorite to possess less than half (5·44 %) of its original water content. Dehydration of the normal 14 Å chlorites appears to occur in two distinct stages. Much of the 'water' is lost at about 600° C, with the accompanying endothermic reaction; and the remaining OH is largely retained to about 800° C where its loss accompanies and may even trigger the structural breakdown. Replacement of OH′ ions by O″ ions would, of course, create electrostatic disequilibrium and, hence, structural instability. The two-stage dehydration observed in the 14 Å chlorites is presumably related to the two possible sites in which OH′ ions may occur. The OH′ ions of the 'brucite' layer should be more easily removed than those buried deep within the 'mica' layer. Dehydration of the 7 Å septechlorites seems to occur in a single stage immediately preceding the structural collapse. Amesite, here called septeamesite, from the Chester, Massachusetts, locality has been described as a mixed-layer structure of the 14 Å and 7 Å types. Such a structure might be responsible for the double endothermic peak, but the presence of a 14 Å unit is not apparent from X-ray powder patterns.

Coincidence of the exothermic structure change and endothermic dehydration frequently produces a complex curve in the vicinity of 800° C. The small endothermic peak frequently preceding the 14 Å structural breakdown is presumably caused by the second dehydration stage, and the asymmetrical nature of the exothermic peak may also be attributed to superimposed dehydration.

The major endothermic peak for both 14 Å and 7 Å structures is controlled, in part, by ferrous iron in the chlorite structure. Oxidation of ferrous to ferric iron occurs during the first dehydration stage, and the accompanying increase in positive charge may well help to counteract the negative charge gain of dehydration and restore electrostatic balance. From the D.T.A. curves it is apparent that chlorites high in ferrous iron begin their initial dehydration at appreciably lower temperatures than low-iron chlorites. Iron oxidation with its accompanying exothermic

TABLE III. Analytical data for chlorites (details of specimens in Table I).

	SiO_2	Al_2O_3	Fe_2O_3.*	Cr_2O_3	MgO	FeO	MnO	NiO	CaO†	TiO_2	H_2O†	*Total.*
1 Clinochlore	30·95	19·18	0·87	n.d.	34·05	<0·01	n.d.	n.d.	0·47	<0·10	14·98	100·50
2 Clinochlore	31·85	13·99	1·91	none‡	37·52	<0·01	0·79	none	none	none	13·75	99·81
3 Delessite	32·10	12·01	10·43	n.d.	23·35	n.d.	n.d.	n.d.	11·37†	0·45	10·32	100·03
4 Sheridanite	27·98	25·87	0·61	n.d.	31·10	<0·01	n.d.	n.d.	0·20	<0·10	14·42	100·18
5 Clinochlore	31·19	14·99	3·29	n.d.	33·78	2·08	n.d.	n.d.	0·25	<0·05	14·46	100·04
6 Diabantite	33·18	15·51	2·41	none	19·15	14·92	0·06	none	1·71	1·52	10·31	99·69‖
7 Clinochlore	37·70	13·10	0·77	n.d.	29·70	3·47	n.d.	n.d.	6·45	n.d.	8·75	99·94
8 Kochubeite	30·84	14·47	1·13	3·51	34·59	n.d.	none	0·14	none	none	15·30	99·98
9 Rhodophyllite	26·31	23·92	none	3·90	31·40	1·05	none	0·07	none	none	13·48	100·13
10 Sheridanite	29·48	17·94	3·01	n.d.	33·18	0·88	n.d.	n.d.	0·25	<0·05	15·17	99·91
11 Sheridanite	29·20	20·31	2·10	none	30·03	6·32	0·08	none	none	0·20	12·72	100·96
12 Delessite	36·32	11·64	6·94	n.d.	29·80	0·68	n.d.	n.d.	0·10	0·22	14·07	99·77
13 Ripidolite	26·96	20·53	2·14	n.d.	24·52	13·64	n.d.	n.d.	0·19	1·00	10·94	99·92
14 Diabantite	36·72	12·71	8·20	n.d.	14·87	14·59	n.d.	n.d.	3·37	<0·10	9·61	100·07
15 Corundophilite	24·00	23·24	3·14	none	18·92	15·80	0·94	none	0·05	0·12	12·80	99·01
16 Diabantite	37·11	8·90	3·29	n.d.	11·85	17·35	n.d.	n.d.	8·45†	N.R.	12·78	99·73
17 Ripidolite	24·93	22·69	6·20	n.d.	14·08	21·39	n.d.	n.d.	0·38	<0·10	10·01	99·68
18 Aphrosiderite	23·63	21·68	4·92	none	11·11	27·19	none	none	0·05	0·15	11·82	100·55
19 Aphrosiderite	24·72	19·94	6·05	none	4·95	31·60	0·84	none	0·46	0·40	10·72	99·68
20 Daphnite	28·15	17·36	3·08	none	4·66	33·44	0·28	none	0·98	0·31	9·60	99·43§
21 Klementite	24·84	17·84	20·18	none	10·12	15·88	0·43	none	0·05	none	11·46	100·80
22 Septekämmererite¶	50·70	3·17	none	0·61	33·51	1·07	none	0·32	0·10	none	11·00	100·48
23 Antigorite...	41·90	2·50	2·05	none	36·70	4·26	none	0·11	none	none	12·81	100·33
24 Septekämmererite	34·16	9·41	0·80	5·07	36·35	<0·01	none	0·42	none	none	13·17	99·41**
25 Septeamesite	21·13	34·45	1·58	N.R.	23·47	7·57	N.R.	N.R.	0·25	<0·10	11·84	100·29
26 Septeaphrosiderite	16·42	19·75	0·46	none	3·28	32·40	0·38	none	4·06†	0·15	7·15	98·24††

peak appears to occur quite consistently at about 610° C, as shown by chemical analysis. For chlorites very high in ferrous iron, dehydration occurs between 500° C and 600° C, and a small exothermic peak immediately follows the large endothermic one. For moderate-iron chlorites, oxidation is superimposed on the large endothermic peak flattening the slope on the 610° C side. The dehydration is usually symmetrical when 610° C is at its apex or for very low-iron chlorites and very high-iron chlorites where 610° C is beyond the limits of the endothermic curve.

Although the amplitude of the various peaks is not considered to be very reliable, it may be significant to note the large undulations produced by the septechlorites and the small amplitudes of the diabantite curves.

It may also be of value to note here the confirmation of the work of Dschang[1] and others which leads to the conclusion that ferrous iron may be oxidized within the chlorite structure in accordance with the equation $Fe'' + OH' - Fe''' + O''$. However, the proposal of A. N. Winchell[2] that

[1] G. L. Dschang, Chemie der Erde, 1931, vol. 6, p. 416.
[2] A. N. Winchell, Amer. Journ. Sci., 1926, vol. 11, p. 283.

---

* Fe_2O_3 is total iron, where FeO was not determined.

† In author's opinion CaO and alkalis are not appropriate in a chlorite analysis, and these oxides were deducted and every analysis recalculated to 100 % for classification. Numbers 3, 16, and 26 contain too much CaO to be held as cation exchange. Number 3 was not prepared for analysis by the author, and the entire sample was used in the analysis. The source of the CaO is, therefore, unknown. Number 16 was also not prepared by the author, and subsequent examination of the sample as submitted for analysis showed large amounts of tremolite. By counting in a thin section of the sample, the sample was judged to contain 31·5 wt. % tremolite (assuming an iron-free tremolite of density 2·98 and a measured density of 2·66 for the chlorite). Heavy liquid (bromoform) separation on the analysed sample produced 30 wt. % tremolite, and the classification was made on the above analysis with 31 % theoretical tremolite deducted. Purification of number 26 was very difficult, and the sample as submitted for analysis was known to contain carbonates. The analysis showed 13·95 % CO_2. This was combined with all of the CaO (4·06 %) and much of the FeO (17·54 %), and the analysis recalculated to 100 % for classification.

‡ Checked spectrographically.

‖ Contains 0·92 % K_2O.

§ Contains 0·56 % K_2O, 0·28 % Na_2O, and 0·73 % P_2O_5.

¶ X-ray diffraction shows this specimen to be a septechlorite, but the chemica analysis is invalid for a chlorite. This sample was leached with hot HCl prior to chemical analysis to remove dolomite impurities. The anomalous analysis is attributed to this leaching which must have resulted in an appreciable loss of trivalent ions. The D.T.A. curve, however, was obtained with an unleached portion of the sample free of dolomite.

** Contains 0·03 % P_2O_5.

†† Contains 13·95 % CO_2, 0·09 % Cl, and 0·15 % S.

all ferric iron occurring in a chlorite was originally ferrous and should be recalculated to ferrous iron for purposes of classification, is completely rejected by this writer. If all ferric iron resulted from the natural oxidation of ferrous iron after the chlorite formation, we should expect chlorites rich in ferric iron to be correspondingly poor in water. This is not confirmed by observation, and much of the ferric iron can be shown to have been necessary for electrostatic balance when the chlorite was formed. Even if one allows that oxidation could and does take place, it is inappropriate to ignore the fact that it has done so; since chlorites are themselves alteration minerals, it is certainly appropriate to supply variety names for the ferric-iron chlorites.